Optimizing Storage Siting, Sizing, and Technology Portfolios in Transmission-Constrained Networks

Sonja Wogrin, *Member, IEEE*, and Dennice F. Gayme, *Senior Member, IEEE*

***Abstract*—In this paper, we propose a DC optimal power flow (OPF) framework for storage portfolio optimization in transmission-constrained power networks. In particular, this model is designed to investigate two problems: 1) optimizing storage operation and allocation over a network given a fixed technology portfolio and 2) optimizing the storage portfolio (i.e., the size, technology, and network allocation of these resources). We demonstrate this framework using case studies based on the IEEE 14-bus test system with four different storage technologies. Our results show that although certain technologies are generally classified as being suitable for either power or energy services, many technologies can add value to the system by performing both fast-time scale regulation (power) and load-shifting (energy) services. These results suggest that limiting the type of service that a certain technology is compensated for may result in inefficiencies at the system level and under-valuation of storage.**

***Index Terms*—Electric power grid, energy storage, linear programming, optimal power flow, optimization.**

I. Introduction

GRID-SCALE energy storage has the potential to provide the grid flexibility needed to accommodate a high penetration of non-dispatchable power sources (e.g., solar and wind). Early research into grid integration of large-scale energy storage focused on peak shaving, energy arbitrage, and power regulation [1]. Recent studies have also investigated the use of energy storage for ancillary services such as frequency support, contingency reserves, and black-start [2] as well as to augment or replace fast-ramping generation resources [3]. Economic questions such as the use of storage to defer transmission or capacity investments also represent a growing area of energy storage research, see, e.g., [4].

Grid-scale storage encompasses a number of technologies that cover a wide range of time-scales, costs, spatial footprints, and capacity. Identifying the appropriate size, siting, and technology is important for realizing the full potential of storage in renewable energy integrated power grids. Many of these questions are application dependent, and therefore, research related to storage capacity requirements has often focused on specific problem settings. For example, isolated systems with high renewable energy penetration have been investigated in a number of contexts, e.g., [5]–[7]. Other studies have focused on characterizing the amount of storage required to compensate for short- [3] and long-term [8] energy deficits and to replace fast response generators in single bus systems.

In a network setting, both capacity requirements and the allocation of storage resources strongly depend on the network properties. One of the most common ways to include network effects is through the optimal power flow (OPF) framework, which optimizes a cost function subject to physical and operational constraints on both the network and at the individual buses (network nodes). OPF with storage formulations have been proposed for operational, siting, and sizing problems, see, e.g., [9]–[14]. However, the general OPF with storage problem (as well as the basic OPF) is difficult to solve because it is a nonconvex, NP hard problem. The DC OPF [15]is a linear approximation of this problem, see, e.g., [15], [16] for a review of DC OPF formulations, which has been extensively used to investigate optimal storage siting in both conventional and renewable energy integrated systems, see, e.g., [17]–[20].

Much of this growing literature on storage siting assumes a single technology with a fixed maximum capacity. However, as previously discussed, the variety of storage options means that a combination of technologies may be more effective than any single storage modality in mitigating the multi-scale issues that arise in renewable energy applications. Selecting an appropriate portfolio of technologies was the topic of [21], which investigates optimization methods for choosing a candidate portfolio of storage devices. Kintner-Meyer *et al.*[22] similarly assess sizing requirements for a portfolio of resources including fast-ramping conventional resources, batteries, pumped hydro energy storage, and demand response for energy arbitrage and load-balancing in the western part of the United States, in particular the area governed by the Western Electricity Coordinating Council (WECC). This study was later extended to the national level [23]. A related report augmented these findings with assessments of economic factors affecting storage investment including an analysis of the relationships between storage performance and various storage system costs [24]. However, none of these studies considered network effects as [21] used a model based on a single bus system and the analyses performed in [22]–[24] aggregated the loads into balancing areas.

There have been few studies that investigate co-optimization of storage allocation, sizing, and the storage technology portfolio over a network. The present work takes a step toward bridging this gap by co-optimizing siting and sizing of a

Manuscript received June 20, 2014; revised September 24, 2014; accepted December 01, 2014. Date of publication December 22, 2014; date of current version August 03, 2015. This work was supported in part by the National Science Foundation, grant number IIA-1243482 (the WINDINSPIRE project). Paper no. TPWRS-00838-2014.

S. Wogrin is with the Institute for Research in Technology, ICAI School of Engineering, Comillas Pontifical University, 28015 Madrid, Spain (e-mail: Sonja.Wogrin@iit.upcomillas.es).

D. F. Gayme is with the Department of Mechanical Engineering, Johns Hopkins University, Baltimore, MD 21212 USA (e-mail: dennice@jhu.edu).

Digital Object Identifier 10.1109/TPWRS.2014.2379931

storage technology portfolio consisting of four technologies in a transmission-constrained network. The contributions of this work are as follows. The work extends previous DC OPF-based storage allocation formulations (e.g., [17], [19]) to include multiple storage technologies with different operational time-scales into the OPF-based storage siting and dispatch problems. This formulation is then used to investigate how this decision might be affected if regulatory measures were to require that the cost function include penalties for cycling or other life-cycle costs associated with a particular technology, i.e., a so-called life-cycle payment. The second main contribution of this work is an extension of this storage allocation framework to investigate the optimal types, sizes, and siting given a candidate storage portfolio. We refer to this as the *storage investment problem* as it determines the storage capacity and technology mix one needs for optimal operation of a given system. The basic modeling framework is detailed for a deterministic problem setting, but extensions that include uncertainty and stochastic problem settings are also presented. The basic (deterministic) version of both problem settings are explored through case studies that serve to illuminate the driving factors for each of these decisions under various network conditions.

The remainder of this paper is organized as follows. Section II provides mathematical formulations for optimizing storage dispatch and siting across a transmission-constrained network. Section II-A provides the basic framework, which is extended to incorporate life-cycle costs in Section II-B and technology portfolio optimization in Section II-C. The effect of uncertainty is addressed in Section II-D, which describes several approaches to extending the model to a stochastic problem setting. Section III presents case studies illustrating the use of the modeling framework for an IEEE benchmark test system under a number of different conditions. Sections III-B–III-C investigate storage allocation in a nominal network and one with binding transmission constraints. Section III-D examines the effect of life-cycle payments. Then, the case studies in Sections III-E–III-F investigate the complementary problem of selecting the optimal storage technology portfolio, i.e., the optimal storage investment given a pre-determined portfolio of technologies. Conclusions and directions for future work are presented in Section IV.

II. Methodology—Problem Formulation

This section contains the mathematical formulations for optimal storage allocation over a transmission-constrained network. These models extend the OPF with storage problem to include multiple storage technologies, which greatly increases the problem size. Therefore we linearize the problem using a DC OPF approximation in order to retain a tractable problem with a provably optimal solution. The first model, presented in Section II-A, assumes a fixed total storage capacity for a portfolio of technologies and optimizes storage allocation of the available resources over a transmission network. In Section II-B, this model is extended to take into account storage cycling and life-cycle costs using so-called life-cycle payments. Finally, Section II-C further extends the framework to optimize storage capacity given a fixed portfolio of storage technologies.

A. Storage Allocation

Consider a network with a set of buses $\mathcal{N} := \{1, \ldots, N\}$ and define n as the index referring to this set. The set of different storage technologies available is denoted by $\mathcal{J} := \{1, \ldots, J\}$, where j represents the index of $\mathcal{J}$. The set of time steps is defined as $\mathcal{T} := \{1, \ldots, T\}$ with index t. The variables of the DC OPF with storage optimization problems are then defined as the set $\Omega := \{p_n^g(t), r_{jn}^c(t), r_{jn}^d(t), s_{jn}(t), k_{jn}, \delta_n(t)\}$ for all storage technologies $j \in \mathcal{J}$, all nodes $n \in \mathcal{N}$ at each time step $t \in \mathcal{T}$. The variable $p_n^g(t)$ corresponds to generation from thermal units, $r_{jn}^c(t)$ and $r_{jn}^d(t)$ represent the charge and discharge rates of each storage technology, $s_{jn}(t)$ corresponds to the storage level, k_{jn} is the installed storage capacity, and $\delta_n(t)$ denotes the voltage angle.

The total system costs are defined in the objective function

$$\min_{\Omega} \sum_{t \in \mathcal{T}} \left\{ \sum_{n \in \mathcal{G}} F_n^g(p_n^g(t), t) + \sum_{n \in \mathcal{N}, j \in \mathcal{J}} F_{jn}^d(r_{jn}^d(t), t) \right\} \quad \text{(1a)}$$

which is the sum of the production costs $F_n^g(p_n^g(t), t) := C_n^{g1}(t) p_n^g(t) + C_n^{g2}(t)(p_n^g(t))^2$ and the discharge costs $F_{jn}^d(r_{jn}^d(t), t) := C_{jn}^{d1}(t) r_{jn}^d(t) + C_{jn}^{d2}(t)(r_{jn}^d(t))^2$, which model operational and maintenance costs of the storage. The parameters $C_n^{g1}(t)$ and $C_n^{g2}(t)$ are respectively the linear and quadratic coefficients of the terms in the production cost function. Similarly, parameters $C_n^{d1}(t)$ and $C_n^{d2}(t)$ are the linear and quadratic coefficients in the discharge cost function.

Let us now describe the constraints of this optimization problem. The energy storage level $s_{jn}(t)\ \forall j, n, t \geq 2$ is

$$s_{jn}(t) = s_{jn}(t-1) + \left(\eta_j^c r_{jn}^c(t) - r_{jn}^d(t)/\eta_j^d\right) \Delta t. \quad \text{(1b)}$$

The energy storage level each node j and time t is thus equal to the storage level at the previous time step, plus the energy charged minus the energy discharged. The energy charged is obtained by the product of charge rate $r_{jn}^c(t)$ and the charging efficiency η_j^c times the duration of the time step Δt. The energy discharged is obtained similarly, by substituting the discharge rate $r_{jn}^d(t)$ and the discharge efficiency η_j^d.

We bound the problem variables as follows:

$$0 \leq r_{jn}^c(t) \leq R_j^c \quad \text{(1c)}$$

$$0 \leq r_{jn}^d(t) \leq R_j^d \quad \text{(1d)}$$

$$0 \leq s_{jn}(t) \leq k_{jn} \quad \text{(1e)}$$

$$s_{jn}(t=1) = s_{jn}(t=T) \quad \text{(1f)}$$

$$P_n^{\min} \leq p_n^g(t) \leq P_n^{\max} \quad \text{(1g)}$$

$$-RR_n \leq p_n^g(t) - p_n^g(t-1) \leq RR_n \quad \text{(1h)}$$

$$k_{jn} = 0 \quad \forall j, n \in GR_{jn} \quad \text{(1i)}$$

$$\sum_{n \in \mathcal{N}} k_{jn} \leq SC_j^{\max}. \quad \text{(1j)}$$

Equations (1c)–(1d) correspond to upper and lower bounds on the charging and discharging rates $\forall j, n, t$, where R_j^c and R_j^d denote the maximum charging and discharging power capacity. Equation (1e) provides lower and upper bounds on the energy storage level $\forall j, n, t$. In (1f), we include a cycling constraint stating that the initial storage level has to be equal to the final

storage level $\forall j, n$, which without loss of generality we can assume to be zero. Constraint (1g) provides lower and upper bounds on generation from thermal units $p_n^g(t)\ \forall n, t$, where $P_n^{\min}$ and $P_n^{\max}$ respectively denote the minimum and maximum thermal power output at node n. Upward and downward ramp rates RR_n on generation from thermal units $\forall n, t \geq 2$ are imposed by constraint (1h). Equation (1i) allows the storage capacity of technology j and node n to be set to zero in order to account for geographical, zoning, or societal issues that may prevent the installation of a particular technology at a particular location as encoded through inclusion in the set GR_{jn}. One example where this constraint would be applicable is when a particular technology, such as pumped storage hydro or compressed air storage, can only be built at nodes that satisfy specific geographical requirements. In that case, all other nodes would be in the set GR_{jn}. Equation (1j) represents an upper bound on the total amount of storage, where $\mathrm{SC}_j^{\max}$ denotes the total available storage capacity of each storage technology j.

At each bus n and each time step t, all power inflows, given by wind production $W_n(t)$, generation from thermal units $p_n^g(t)$, and power discharged from the storage units $r_{jn}^d(t)$ at bus n must be equal to the total power outflows, which are comprised of the demand $D_n(t)$, the power flowing to other buses in the network, and the power $r_{jn}^c(t)$ used to charge storage systems. This power balance is given by

$$D_n(t) + \sum_{m \in \Theta_n} B_{nm}(\delta_n(t) - \delta_m(t)) + \sum_{j \in \mathcal{J}} r_{jn}^c(t) = W_n(t) + p_n^g(t) + \sum_{j \in \mathcal{J}} r_{jn}^d(t). \quad \text{(1k)}$$

Here, the product of the line susceptance between buses n and m, denoted as B_{nm}, and the difference of the voltage angles of these buses, given by $(\delta_n(t) - \delta_m(t))$, model the transmission links in the DC power flow network.

In this formulation, wind production is considered as data and treated as negative load. This straightforward approach has been adopted because in most markets, demand far exceeds wind production and there are often curtailment policies in place to ensure that the wind that is injected into the system never exceeds the system load. However, as wind penetration grows, it may be useful to adjust this framework to account for wind production exceeding demand. Incorporating this situation into the model can be accomplished through replacing the power balance constraint of (1k) with the following two constraints:

$$D_n(t) + \sum_{m \in \Theta_n} B_{nm}(\delta_n(t) - \delta_m(t)) + \sum_{j \in \mathcal{J}} r_{jn}^c(t) = w_n(t) + p_n^g(t) + \sum_{j \in \mathcal{J}} r_{jn}^d(t) \quad \text{(1l)}$$

$$0 \leq w_n(t) \leq W_n(t). \quad \text{(1m)}$$

Here $W_n(t)$ represents total wind production and $w_n(t)$ is a new variable that represents wind production minus any wind curtailment required in order to maintain the power balance in (1l).

In order to introduce transmission line limits, we define the set Θ_n, which denotes the set of buses m connected to bus n at all time steps. These values are bounded $\forall m \in \Theta_n, n, t$ as

$$-TC_{nm}^{\max} \leq B_{nm}(\delta_n(t) - \delta_m(t)) \leq TC_{nm}^{\max}. \quad \text{(1n)}$$

The corresponding voltage angles are bounded as

$$-\pi \leq \delta_n(t) \leq \pi. \quad \text{(1o)}$$

Finally, we set $n = 1$ as the slack bus for all time steps t using

$$\delta_{n=1}(t) = 0. \quad \text{(1p)}$$

The model given by (1a)–(1p) represents an optimization problem with linear continuous constraints and a quadratic objective function. It is a convex problem, and therefore, a provably globally optimal solution can be obtained.

B. Storage Allocation With Life-Cycle Payments

The model presented in the previous section can also be used to assess how potential regulatory measures may impact the solution of the optimal storage allocation problem. A life-cycle payment, for example, can represent the amount of money that an ISO pays for cycling a particular storage facility to provide services such as frequency regulation, power quality, and voltage stability. Such payments may, for example, help compensate storage purveyors for the costs associated with reduced life expectancy of a technology due to a finite number of duty-cycles and can equalize costs between technologies that have vastly different cycling capacity or life expectancy. This type of measure can be easily incorporated into the optimization problem in (1a)–(1p) by adding the following "life-cycle payment" term to the objective function in (1a):

$$\sum_{t \in \mathcal{T}} \sum_{n \in \mathcal{N}, j \in \mathcal{J}} MP_j o_{jn}(t) \quad \text{(2)}$$

along with the constraints

$$\left(s_{j,n}(t) - s_{j,n}(t-1)\right)/\Delta_t \leq o_{jn}(t) \quad \text{(3)}$$

$$\left(s_{j,n}(t-1) - s_{j,n}(t)\right)/\Delta_t \leq o_{jn}(t). \quad \text{(4)}$$

In the life-cycle payment term of (2), MP_j represents the life-cycle payment in [$/MW] and $o_{jn}(t)$ denotes the absolute value of the change in the storage level. The constraints (3)–(4) define the life-cycle of each technology j at each bus n and each time step t.

C. Storage Investment and Allocation

We now extend the model of Section II-A, which assumes a fixed available capacity for each storage technology to include an investment decision. This storage investment optimization problem is given by

$$\min_{\Omega} \sum_{t \in \mathcal{T}} \left\{ \sum_{n \in \mathcal{G}} F_n^g(p_n^g(t), t) + \sum_{n \in \mathcal{N}, j \in \mathcal{J}} F_{jn}^d(r_{jn}^d(t), t) \right\} + \sum_{n \in \mathcal{N}, j \in \mathcal{J}} F_j^i(k_{jn}) \quad \text{(5a)}$$

$$\text{s.t. (1b)} - \text{(1i)}, \text{(1k)} - \text{(1p)}. \quad \text{(5b)}$$

The differences of this model with respect those presented in Sections II-A and II-B are as follows: the upper bound (1j) on capacity k_{jn} has been omitted; in the objective function (5a), the total system costs are calculated as the sum of production and discharge costs as in the previous section plus an additional term corresponding to the storage investment costs defined as $F_j^i(k_{jn}) = k_{jn}C_j^i/\mathrm{DD}_j$, where C_j^i corresponds to the per MW investment cost of a storage technology and DD_j represents the average discharge duration of the technology. The rest of the constraints as well as the set of variables Ω remain unchanged.

Equations (5a)–(5b) also define a convex optimization problem with linear constraints and a quadratic objective function. In reality, capacity investments are discrete. In our model, capacities k_{jn} are considered continuous variables in order to keep the formulation simple. Therefore, it could occur that the total new storage capacity built in each storage technology does not coincide with realistic, lumpy sizes of storage units. It is possible to consider discrete investment decisions in our model. This modification, however, requires the introduction of binary variables yielding a quadratic mixed integer optimization problem, which complicates the resolution process greatly. Such a mixed integer formulation can be achieved by introducing the following constraint $\forall j$, where ST_j represents the size (in units of power) of a typical unit of technology j, b_{jn} represent binary variables, and z is the index that helps count the number of units that are built:

$$\sum_n k_{jn} = \mathrm{ST}_j \mathrm{DD}_j \sum_z 2^z b_{jz}. \tag{6}$$

D. Extensions to a Stochastic Problem Setting

The models proposed in this paper provide a modeling framework to analyze the impact of the transmission network on storage siting and investment. This relatively simple deterministic DC OPF-based model provides an important tool for developing intuition as to how various aspects of the problem affect one another. Although this type of simple model is a critical tool for both understanding the problem and guiding further investigations and analysis, a deterministic framework does not capture the inherent uncertainty in grid planning and design decisions in the face of increasingly renewable energy integrated grids. Therefore, one important direction of future work is the extension of this work to include stochastic representations of demand and wind power production. In this section, we outline how such an extension could be carried out. Future research will use the intuition gained in the analysis presented herein to guide additional analysis and numerical case studies that include stochasticity.

The most straightforward way to incorporate uncertainty into our modeling framework would be through a Monte Carlo simulation. This analysis would entail solving the existing models for many different scenarios (random samples) of uncertain parameters such as load, wind production, or variable fuel costs. After many such simulation runs, a probability density of storage investments and allocation can be obtained for further analysis. A more conservative approach would be the use of a chance-constrained OPF problem following the formulations in, e.g., [17], [25], and [26].

Another approach, similar to previous work [27], is to introduce stochasticity directly into the optimization problem. In particular, instead of minimizing a deterministic value of the total system cost in the objective function, one could consider minimizing the expected total system cost, for example, taking into account several different scenarios $\mathcal{B} := \{1, \ldots, B\}$ with index b of uncertain parameters and the corresponding probability PR_b of these scenarios. For the storage investment and allocation problem given by (5), such an extension might lead to a new objective function of the form

$$\min_{\Omega^*} \sum_{b\in\mathcal{B}, t\in\mathcal{T}} PR_b \left\{ \sum_{n\in\mathcal{G}} F_{nb}^g(p_{nb}^g(t), t) + \sum_{n\in\mathcal{N}, j\in\mathcal{J}} F_{jnb}^d\left(r_{jnb}^d(t), t\right) \right\} + \sum_{n\in\mathcal{N}, j\in\mathcal{J}} F_j^i(k_{jn}) \tag{7}$$

along with a new set of variables Ω^*. With the exception of the storage capacity investment variables, all the problem variables would then depend on the new index b. The corresponding constraint set would parallel that of Section II. For the sake of brevity, we have omitted restatement of these constraints.

This establishes the mathematical formulation of the storage allocation and storage investment models of this paper. In the following section, we carry out case studies that demonstrate how these models can be used to provide insight for system planning decisions such as the design and siting of a storage portfolio for a given network.

III. Case Studies

In this section, we present case studies in order to validate the previously presented methodology. Section III-A describes the data for these studies. First, in Section III-B, the storage allocation model of Section II-A is solved assuming an unconstrained network. Subsequently, Section III-C studies the same system with network congestion. Section III-E investigates storage investment decisions using the model in Section II-C.

A. Data

The numerical examples in this section are based on the 14-bus IEEE benchmark system [28], which is depicted in Fig. 1. We add transmission constraints $\mathrm{TC}^{\mathrm{Max}}$ to the nominal network, which unless otherwise stated are set to 400 MW. We consider a time horizon of 24 h in time steps of $\Delta t = 5$ min (leading to a total of 288 time steps). Previous work by Deane *et al.*[29] showed that subhourly time intervals more accurately capture renewable energy variability and the inflexibility in thermal generation units that necessitates the use of storage and other flexible ancillary resources. We selected 5-min time intervals because they also allow us to capture differences in the dispatch and allocation of storage technologies with fast and slow time-scales.

The demand data for these case studies, which is shown in Fig. 2 and whose percentage per node is reported in Fig. 1, represents data of 14 feeders of an average day in Southern California in July of 2010 [11]. This data is provided in 10-min intervals and interpolated to obtain data with time steps of 5 min.

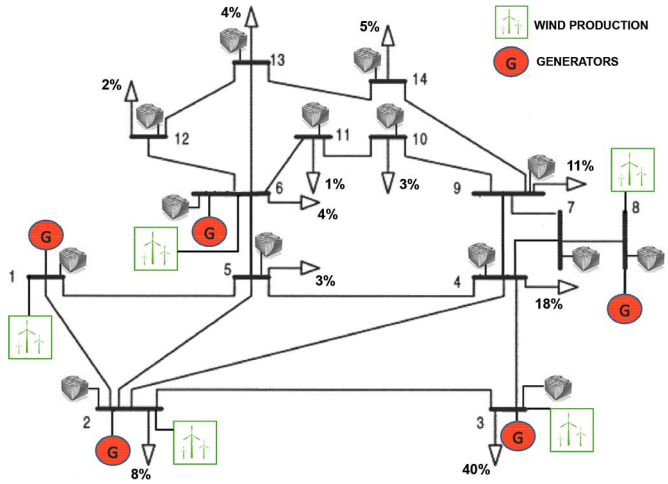

Fig. 1. The 14-bus test network with the wind and conventional generation locations as well as the percent of the total demand at each bus indicated.

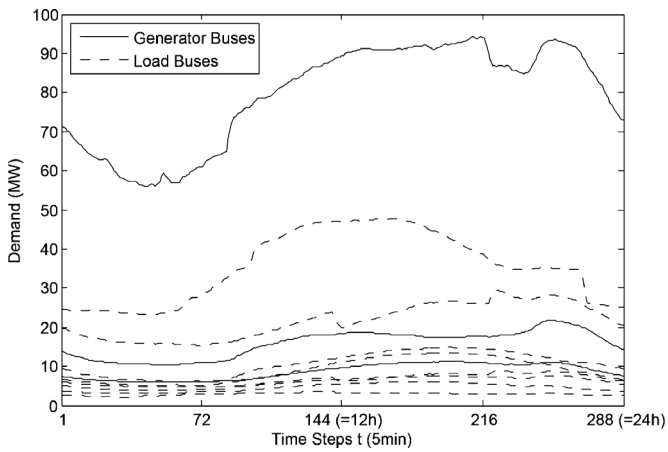

Fig. 2. Total demand at each bus reported at 5-min intervals.

We assume wind production at buses 1, 2, 3, 6, and 8, which are the buses in Fig. 1 that also have conventional generation. The wind data, which is depicted in Fig. 3, is from the 2006 NREL Western Wind Resources Dataset [30]. This wind data is available in 10-min intervals and was also interpolated to obtain 5-min intervals.

We consider four different storage technologies: pumped-storage hydro (PSH), compressed air energy storage (CAES), lithium ion batteries (LI-ION), and flywheel energy storage (FES). Table I contains the charge and discharge efficiencies η^c and η^d, as well as the total available storage capacity $\mathrm{SC}^{\max}$ in MWh and the charging and discharging rates R^c and R^d per time step t for each of these storage technologies. The charging and discharging efficiencies as well as the charging and discharging rates in Table I are assumed to be equal and are based on [31]. The storage capacity, given in Table I, has been obtained by considering the minimum capacity (MW) of a unit of each technology and a typical discharge duration (h), both of which have been based on the information given in [32]. The technical information regarding FES, however, has been obtained from [33] and represents a cluster of ten flywheel modules (each with a capacity of 1.5 MW, an energy delivery of

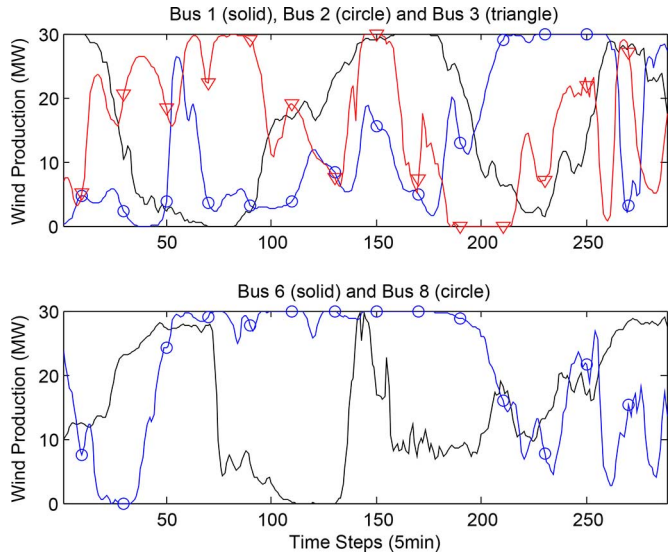

Fig. 3. Wind production at each of the wind buses shown in Fig. 1.

TABLE I
STORAGE DATA

Storage Technology	Dis-/Charge Efficiency η^c, η^d [p.u.]	Total Storage Capacity SC^{max} [MWh]	Dis-/Charging Rates R^c, R^d [MW]
PSH	0.87	3000	250
CAES	0.78	360	15
LI-ION	0.94	20	5
FES	0.96	1.25	15

125 kWh, and a discharge time of 5 min). In what follows, each FES module is assumed to consist of ten individual flywheels.

The operational cost of charging is equal to the locational marginal price (LMP) at the bus. The operational cost of discharging is considered to be zero; however, there exists the option to include operation and maintenance costs. The operational costs of the thermal generators are $C_n^{g1} = 20$ [\$/MW] for buses $n = \{1, 2\}$ and $C_1^{g2} = 0.043, C_2^{g2} = 0.25$ [\$/MW^2]. At buses 3, 6, and 8, the thermal generators are more expensive, which leads to linear production cost coefficients of $C_n^{g1} = 40$ [\$/MW] and $C_n^{g2} = 0.1$ [\$/MW^2] for $n = \{3, 6, 8\}$. The lower bound on generation from thermal units $P^{\min}$ at all generator nodes is zero and the upper bound in MW is given by $P_1^{\max} = 332.4, P_2^{\max} = 140$ and by $P^{\max} = 100$ for the rest of the buses. We assume all of the conventional generators have ramp rates $RR = 2$ MW per 5-min time step.

All of the problems in Section III are solved numerically using the CPLEX solver in GAMS [34]. For the network considered, these problems consist of about 65 000 variables with 160 000 equations and take between 7 and 13 s to solve on a 2.30-GHz Intel(R) Core(TM) with 4 GB of RAM.

B. Storage Allocation

The optimal solution of storage allocation problem (1a)–(1p) with no transmission constraints is equal allocation of the total available capacity $\mathrm{SC}^{\max}$ [MWh] at each bus, i.e., the storage at each bus is $k_{jn} = SC_j^{\max}/14$. This result is not surprising as the lack of network congestion means that the LMPs are equal, and therefore, there are no preferential storage sites as discussed in [12]. The black continuous line in Fig. 4 represents the total net

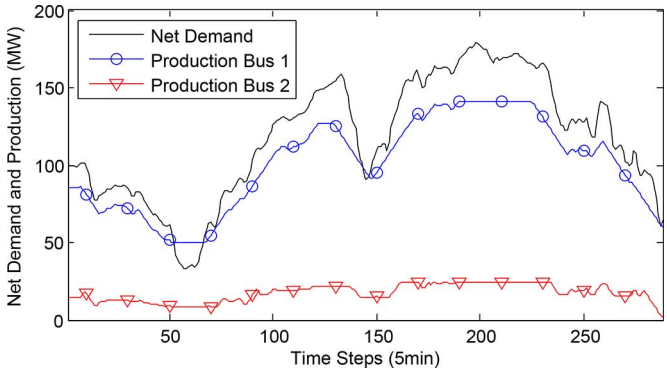

Fig. 4. Total net demand in the system (demand − wind production) compared with the generation at buses 1 and 2 over the 24-h time horizon.

demand (demand − wind production) of the entire system and the blue and red lines show the generation from thermal units at the two buses with the cheapest generation (buses 1 and 2). It can be observed that due to the wind production, the relatively smooth demand curves of Fig. 2 have become considerably less smooth; however, the general trends of low demand during the night time hours and high demand during the day time hours are maintained.

Fig. 5 compares the net demand (demand − wind production) with the storage levels $s_{jn}(t)$ for each storage technology over the entire time horizon. The available CAES capacity is not used in this simulation, due to its low round-trip efficiency, and therefore, it has been omitted from Fig. 5. The PSH storage facilities charge when net demand is lowest, which corresponds to the times at which the LMPs are also smallest. They then keep their energy level constant until discharging when prices are highest (net demand is highest). This behavior is commonly known as energy arbitrage. The FES systems are capable of charging and discharging their entire capacity in only one time step and therefore tend to be used to balance short-term fluctuations due to wind production. In contrast to the PSH, which exhibits a single charge/discharge cycle over the course of the entire time horizon, the FES modules have several charging cycles per day. The LI-ION battery behaves like a mix of the PHS and FES. On the one hand, the overall storage level resembles the PSH curve, where it charges to full capacity in the morning hours when energy is cheap and discharges completely when prices are highest. However, the LI-ION storage facilities also react to short-term drops in net demand (for example around time step 150). From a technical perspective, it seems that LI-ION batteries can do both energy arbitrage and short-term balancing, even though they might only be compensated for one of these services.

C. Storage Allocation Under Congestion

Let us now analyze how the results of the previous section are affected by adding congestion to the network. To that purpose, we set $\mathrm{TC}_{12}^{\max} = 80$ MW, $\mathrm{TC}_{15}^{\max} = 40$ MW, $\mathrm{TC}_{23}^{\max} = TC_{45}^{\max} = 30$ MW and continue to impose a line capacity of 400 MW on the remaining lines. Essentially, this means that when demand gets too high, the two cheapest thermal generators, located at buses 1 and 2, are isolated from the rest of the system and especially from the high demand buses 3 and 4.

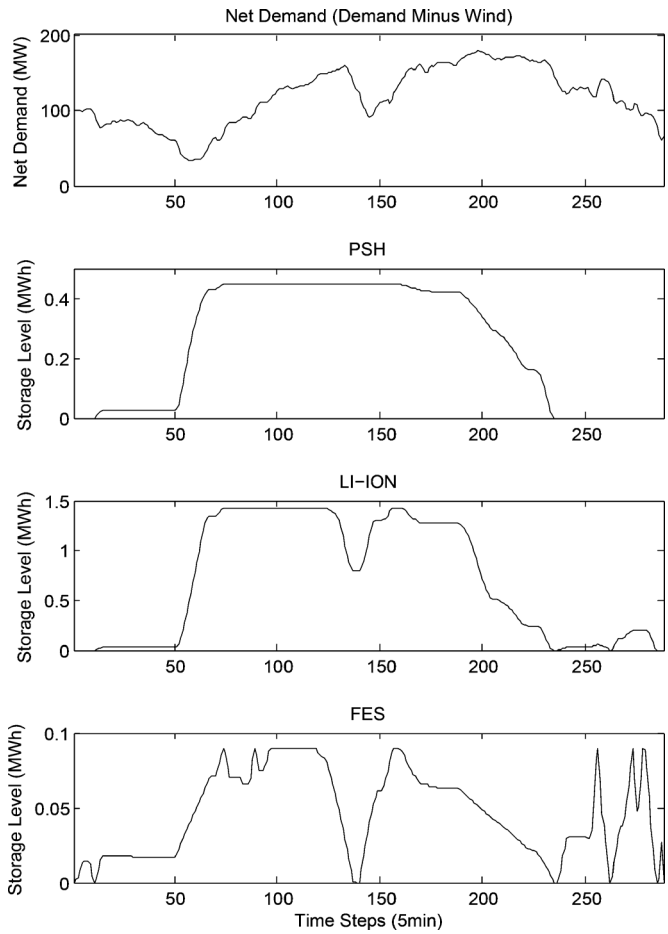

Fig. 5. Total net demand in the system (demand − wind production) and storage level at each bus for different storage technologies over the time horizon.

The first observation we make from the results of the optimization for the transmission-constrained network is that network congestion has a huge impact on storage allocation. In the previous section, the total storage capacity was equally spaced among all of the buses in the system. Now, however, this has changed. PSH for example places around 7% of its capacity at all buses, except for buses 3 and 4, where we observe a slightly elevated capacity of 7.5% and 8.5%, respectively. Since CAES is not used at all (due to the same reasons as in the previous section), its total capacity is equally spaced over all buses of the system. A very drastic change can be observed among the LI-ION batteries; 92% of the capacity is placed at bus 3, 7% are placed at bus 4, and less than 1% is assigned to bus 2. Finally, 60% of the capacity of FES is placed at bus 3, 20% is located at bus 4, and another 20% is installed at bus 2. These results indicate that network congestion is an important driver of storage allocation.

Fig. 6 contains the storage levels at each of the buses where storage facilities are actually used. PSH is operated only at buses 3 and 4, which account for about 60% of the total system demand. We furthermore observe that the active PSH capacity is located just at the border of the congested region formed by buses 1 and 2 where the inexpensive thermal generators are located. From buses 3 and 4, the PSH facilities can cater to the rest of the system (buses 5 to 14) where there is little congestion

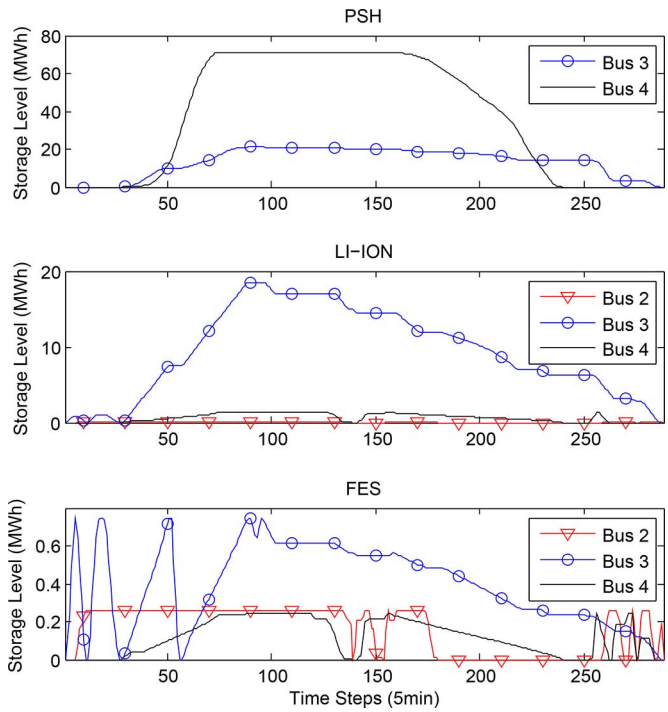

Fig. 6. Storage level with congestion at active buses for different storage technologies over the 24-h time horizon.

during the high net demand (and high price) time steps. Contrary to common conjectures expressed in the literature, storage capacity is not highest at wind producing buses. In our case, there is no wind production at bus 4, while PSH is predominantly located as bus 4. Similarly, even though demand is highest at bus 3, PSH usage is not highest at bus 3. It is actually highest at bus 4 because of the congestion on line 2–3 and the fact that line 2–4 has not reached its capacity limit. FES capacity is also predominantly placed at buses 3 and 4 outside the congested region in order to balance instabilities of the rest of the system. We also observe that there is a small amount of FES capacity at bus 2, within the congested region, which helps to mitigate short-term fluctuations due to wind production at buses 1 and 2. While energy-driven storage like PSH is operated solely from outside the congested region to cover the system demand, fast-reacting storage technologies such as FES are operated on both sides of the congested lines because wind production causes short-term imbalances in both of these areas. As in the unconstrained network discussed in Section III-B, LI-ION batteries seem to perform both power and energy services. The LI-ION technology is more flexible than PSH but still allocates 99.5% of its capacity at buses 3 and 4, just like PSH; however, a very small amount of capacity is also placed at bus 2. In conclusion, it can be said that network congestion is a fundamental driver of storage allocation but there is some dependency on the type of storage technology.

Even when considering the DC linear approximation of the optimal power flow constraints, which does not consider network losses, it can be observed that storage allocation is affected by congestion. In [35], the authors show that the optimal storage operational strategy and storage allocation obtained via a DC

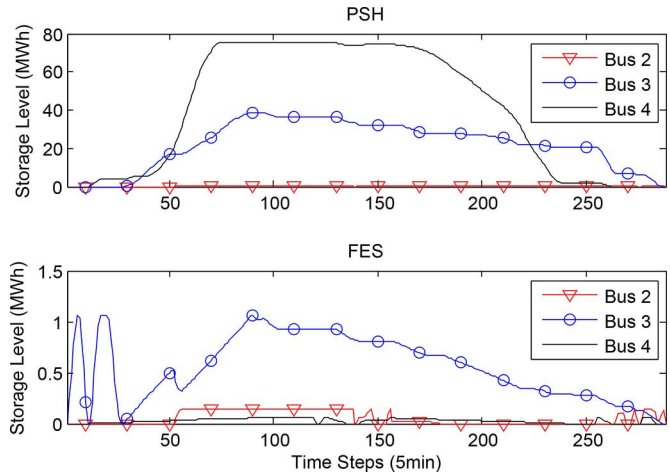

Fig. 7. Storage level with congestion and life-cycle payment at active buses of each different storage technology over the time horizon.

OPF with storage problem that includes losses can be quite similar to those of the full AC optimal power flow. Hence, in future research, an approximation of network losses could be included in the models presented in this paper, in order to assess the additional influence that losses might have on storage allocation.

D. Storage Allocation With Congestion and Life-Cycle Payments

In this section, we repeat the analysis of Section III-C in the extended problem setting described in Section II-B, which includes additional cost function terms and constraints associated with life-cycle payments. We assume a life-cycle payments MP of 0.4 $/MW for both PSH and CAES, 1 $/MW for FES, and 5 $/MW for LI-ION.

Fig. 7 contains the results of this case. As neither LI-ION nor CAES is used in the optimal solution, they are omitted in the figure. The results imply that the life-cycle payment for LI-ION batteries is too high to actually make their operation profitable. The remaining storage technologies, however, are used to a greater extent. For example, the maximum PSH storage level at bus 3 is almost twice as high as in the case without life-cycle cost. There even is a small increase of PSH usage at bus 4 and 2. Since LI-ION no longer provides energy arbitrage services, the opportunity for PSH is higher. The same can be observed for FES, where at bus 3, the maximum storage level increases for about 20%.

The changes in allocation of the PSH is an increase to 7.7% at bus 3 while all other buses remain the same. The FES allocation changes more drastically. Now 85% of the capacity is located at bus 3, 11% at the other side of the congested lines at bus 2, and only 4% remain at bus 4. As demonstrated by the results, this type of payment not only alters the way in which storage technologies are used, but it also has an impact on the actual allocation of storage within the network.

E. Storage Investment

When solving the storage investment model, given by (5a)–(5b), we not only obtain the optimal allocation of storage but also the optimal investments for each storage technology. In

TABLE II
INVESTMENT DATA

Storage Technology	Investment Cost C^i [€/MW/day]	Discharge Duration DD [h]	Capacity Step Size ST [MW]
PSH	250	12	250
CAES	50	24	15
LI-ION	800	4	5
FES	550	1/12	1.5

previous case studies, the storage portfolio and corresponding storage capacities are considered data and hence predetermined. The investment model, however, decides the optimal storage portfolio and the total optimal capacity for the given system and can therefore be used as a planning tool.

The additional parameters required for the investment model are shown in Table II. Here both the investment cost C_j^i and the average discharge duration DD_j of each storage technology are based on [32]. We can use our model on an arbitrary time frame. In this case study, however, we consider a time horizon of one day and we hence have to scale down the investment costs C_j^i to one day. In particular, the investment costs presented in Table II are obtained by taking the total capital cost of each storage technology and dividing it by the lifetime (in days), both of which are given in [32]. Table II also contains the typical size (in power) of a single unit of each technology. The rest of the data and parameters are the same as in Section III-B, i.e., no congestion is considered.

In the optimal solution obtained using these parameters, neither CAES nor FES storage is installed—CAES due to its low round trip efficiency and FES due to its high investment cost. There is, however, a total investment of 12.7 MWh in PSH and 1.0 MWh in LI-ION, uniformly distributed among the 14 buses of the network. In comparison to $\mathrm{SC}^{\max}$ of Section III-B, this amount is a lot smaller due to the fact that now investment costs also have to be taken into account.

Fig. 8 shows the optimal storage levels of PSH and LI-ION. A comparison of this figure with Fig. 5 illustrates that the LI-ION batteries replace the unavailable FES in balancing short-term (faster-time scale) power fluctuations in the system. The behavior of PSH resembles the previous behavior of LI-ION. In the allocation problem, both PSH and LI-ION capacity were readily available, and hence, PSH could focus on energy arbitrage only. Now, LI-ION has taken over the balancing behavior of FES, and it no longer provides energy arbitrage. Therefore, PSH has to provide both—the energy arbitrage service and flexibility for when wind suddenly drops or appears.

F. Storage Investment With Congestion

Applying the same network constraints as in Section III-C leads to network congestion, which increases the value of storage facilities. In particular, 114 MWh of PSH and 2 MWh of LI-ION batteries are built. Again it seems that the efficiency of CAES is too low and the assumed investment cost for FES is too high to trigger investment in these technologies.

Similar to Section III-C, PSH capacity is allocated at buses 3 (29.4%) and 4 (70.6%). LI-ION capacity is placed at buses 2 (8.4%), 3 (63.5%), and 4 (28.1%) of the network. However, the capacity is notably higher at the high demand buses 3 and 4. Again the LI-ION batteries balance short-term wind-induced fast-time scale fluctuations in the net demand and have several complete charge and discharge cycles per day, as can be seen in Fig. 9.

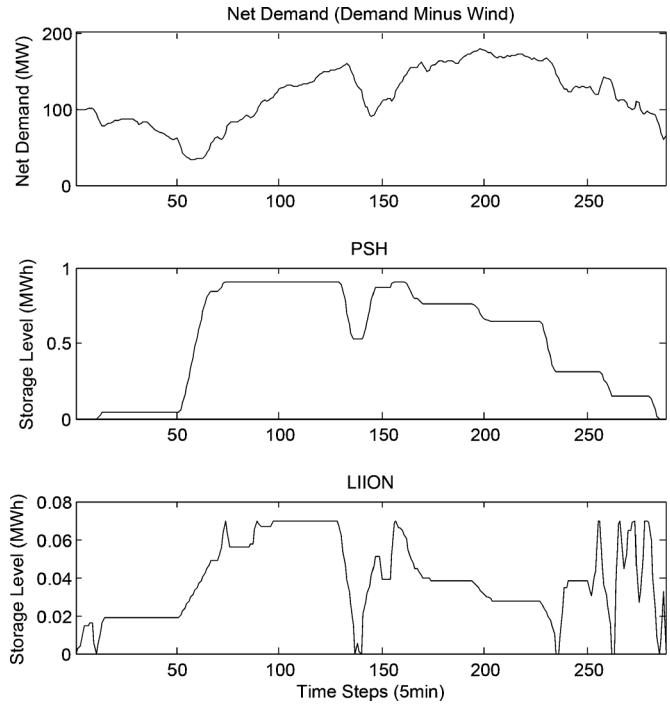

Fig. 8. Storage level with investment and without congestion at each bus.

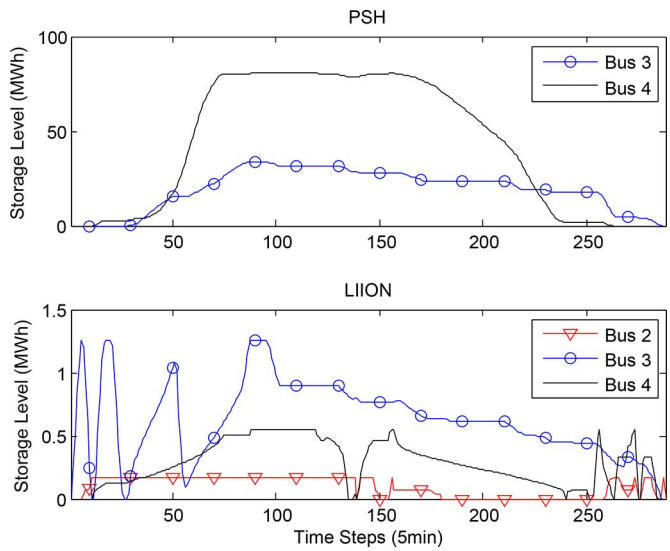

Fig. 9. Storage level with investment and with congestion at each bus.

The case studies discussed above all make use of the deterministic model outlined in Section II-A–II-C. This deterministic framework and small problem sizes allows us to gain insight into how the network drives storage allocation. A similar set of case studies could be performed using the stochastic optimization framework described in Section II-D.

We believe that even though incorporating stochasticity will provide a more accurate estimate of overall storage investments, the main insights obtained from the models presented

in this paper still hold. Although the uncertainty captured by a stochastic problem setting may lead to additional interactions, the basic intuition gained through the analysis contained in this paper is a necessary first step for future research in which stochasticity will be included.

IV. Conclusion

In this paper, we present two models for a transmission-constrained power network with storage, both adopting a DC OPF framework. The first model decides optimal siting and operation of the storage given a fixed portfolio of different storage technologies. The second model extends this framework to also optimize the storage technology mix, new storage capacity investments, and the network allocation of these resources. We furthermore show how life-cycle payments (e.g., to account for cycling and other operational costs) can be included in the formulations. Both models are demonstrated in different case studies using the topology of the IEEE 14-bus benchmark system. The results indicate that storage allocation is mainly driven by the network properties. However, we also observe that storage allocation is affected by the type of storage technology. In particular, energy-based technologies such as pumped hydro storage tend to be allocated at the main demand nodes, whereas power-based storage technologies such as flywheels are optimized when co-located with wind. However, depending on the congestion in the system and the existing storage technology mix, storage technologies can also adopt a hybrid behavior and cater to both power and energy services.

As discussed above, the modeling framework presented in this paper provides important insight into the factors driving storage placement, portfolio selection, and investment decisions. The case studies highlight critical interactions between features of the network and storage decisions through analyzing problems using this model with an example network and one time series of data. The case studies do not, however, provide a comprehensive study as they are unable to capture a number of issues that are important in real system planning decisions such as the uncertainty in daily wind and load availability. The case studies are also limited to a small number of different storage technologies and only a small sample of wind and load conditions. Although extensions to the model that can capture some of these aspects of the problem are discussed in the problem formulation section of the work, clearly a more detailed model that is specific to the power system of interest would be needed to incorporate all aspects of storage integration. That type of model would however be computationally expensive and lack transparency in evaluating interactions between the various aspects of the problem. Therefore, our framework could serve to complement detailed and stochastic models by providing such insight and helping to determine which aspects of the problems need to be considered simultaneously to capture the crucial interactions involved in studying important planning and investment questions regarding grid scale storage. A combination of modeling approaches and better coordination of these tools are necessary to fully evaluate optimal storage integration in next-generation power systems.

Acknowledgment

The first author would like to thank the WINDINSPIRE program for hosting her Spring 2013 visit to Johns Hopkins University. The authors would also like to thank A. Castillo, B. F. Hobbs, and E. Centeno for many valuable discussions and comments.

References

[1] T. Yau, L. Walker, H. Graham, and A. Gupta, "Effects of battery storage devices on power system dispatch," *IEEE Trans. Power App. Syst.*, vol. PAS-100, no. 1, pp. 375–383, 1981.

[2] H. Ibrahim and A. Ilinca, "Techno-economic analysis of different energy storage technologies," in *Energy Storage-Technologies and Applications*. Rijeka, Croatia: InTech, 2013, pp. 1–40.

[3] H.-I. Su and A. El Gamal, "Modeling and analysis of the role of fast-response energy storage in the smart grid," in *Proc. 49th Allerton Conf. Communication, Control and Computing*, 2011, pp. 719–726.

[4] P. Denholm and R. Sioshansi, "The value of compressed air energy storage with wind in transmission-constrained electric power systems," *Energy Policy*, vol. 37, no. 8, pp. 3149–3158, 2009.

[5] P. Denholm and M. Hand, "Grid flexibility and storage required to achieve very high penetration of variable renewable electricity," *Energy Policy*, vol. 39, no. 3, pp. 1817–1830, 2011.

[6] K. M. Chandy, S. Low, U. Topcu, and H. Xu, "A simple optimal power flow model with energy storage," in *Proc. 49th IEEE Conf. Decision and Control*, 2010, pp. 1051–1057.

[7] P. Brown, J. P. Lopes, and M. Matos, "Optimization of pumped storage capacity in an isolated power system with large renewable penetration," *IEEE Trans. Power Syst.*, vol. 23, no. 2, pp. 523–531, May 2008.

[8] H. I. Su and A. E. Gamal, "Modeling and analysis of the role of energy storage for renewable integration: Power balancing," *IEEE Trans. Power Syst.*, vol. 28, no. 4, pp. 4109–4117, Nov. 2013.

[9] D. F. Gayme and U. Topcu, "Optimal power flow with large-scale storage integration," *IEEE Trans. Power Syst.*, vol. 28, no. 2, pp. 709–717, May 2013.

[10] Y. M. Atwa and E. F. El-Saadany, "Optimal allocation of ESS in distribution systems with a high penetration of wind energy," *IEEE Trans. Power Syst.*, vol. 25, no. 4, pp. 1815–1822, Nov. 2013.

[11] S. Bose, D. Gayme, U. Topcu, and K. Chandy, "Optimal placement of energy storage in the grid," in *Proc. 51st IEEE Conf. Decision and Control*, 2012, pp. 5605–5612.

[12] A. Castillo and D. F. Gayme, "Profit maximizing storage allocation in power grids," in *Proc. 52nd IEEE Conf. Decision and Control*, 2013, pp. 429–435.

[13] A. Gopalakrishnan, A. U. Raghunathan, D. Nikovski, and L. T. Biegler, "Global optimization of multi-period optimal power flow," in *Proc. American Control Conf.*, 2013, pp. 1157–1164.

[14] Z. Hu and W. T. Jewell, "Optimal power flow analysis of energy storage for congestion relief, emissions reduction, and cost savings," in *Proc. 2011 IEEE/PES Syst. Conf. Expo.*, 2011.

[15] K. Purchala, L. Meeus, D. Van Dommelen, and R. Belmans, "Usefulness of DC power flow for active power flow analysis," in *Proc. IEEE PES General Meeting*, 2005, pp. 2457–2462.

[16] B. Stott, J. Jardim, and O. Alsaç, "DC power flow revisited," *IEEE Trans. Power Syst.*, vol. 24, no. 3, pp. 1290–1300, Aug. 2009.

[17] A. E. Sjödin, D. Gayme, and U. Topcu, "Risk-mitigated optimal power flow for wind powered grids," in *Proc. Amer. Control Conf.*, Montreal, QC, Canada, Jun. 2012, pp. 4431–4437.

[18] K. Dvijotham, M. Chertkov, and S. Backhaus, "Storage sizing and placement through operational and uncertainty-aware simulations," in *Proc. 47th Hawaii Int. Conf. System Science*, 2014.

[19] C. Thrampoulidis, S. Bose, and B. Hassibi, "On the distribution of energy storage in electricity grids," in *Proc. 52nd IEEE Conf. Decision and Control*, 2013.

[20] M. Ghofrani, A. Arabali, M. Etezadi-Amoli, and M. S. Fadali, "A framework for optimal placement of energy storage units within a power system with high wind penetration," *IEEE Trans. Sustain. Energy*, vol. 4, no. 2, pp. 434–442, 2013.

[21] M. Kraning, Y. Wang, E. Akuiyibo, and S. Boyd, "Operation and configuration of a storage portfolio via convex optimization," in *Proc. IFAC World Congr.*, 2010, pp. 10 487–10 492.

[22] M. Kintner-Meyer, P. Balducci, W. Colella, M. Elizondo, C. Jin, T. Nguyen, V. Viswanathan, and Y. Zhang, National Assessment of Energy Storage for Grid Balancing and Arbitrage: Phase 1, WECC, U.S. Department of Energy, Tech. Rep. PNNL-21388 Phase I, Jul. 2012.
[23] M. Kintner-Meyer, P. Balducci, W. Colella, M. Elizondo, C. Jin, T. Nguyen, V. Viswanathan, and Y. Zhang, National Assessment of Energy Storage for Grid Balancing and Arbitrage: Phase II WECC, ERCOT, EIC, Volume 1: Technical Analysis, U.S. Department of Energy, Tech. Rep. PNNL-21388 Phase II/Vol. 1, Sep. 2013.
[24] V. Viswanathan, M. Kintner-Meyer, P. Balducci, and C. Jin, National Assessment of Energy Storage for Grid Balancing and Arbitrage: Phase II. Volume 2: Cost and Performance Characterization, U.S. Department of Energy, Tech. Rep. PNNL-21388 Phase II/Vol. 2, Sep. 2013.
[25] H. Zhang and P. Li, "Chance constrained programming for optimal power flow under uncertainty," *IEEE Trans. Power Syst.*, vol. 26, no. 4, pp. 2417–2424, Nov. 2011.
[26] D. Bienstock, M. Chertkov, and S. Harnett, "Chance constrained optimal power flow: Risk-aware network control under uncertainty," arXiv:1209.5779, 2013.
[27] S. Wogrin, E. Centeno, and J. Barquín, "Generation capacity expansion in liberalized electricity markets: A stochastic MPEC approach," *IEEE Trans. Power Syst.*, vol. 24, no. 4, pp. 2526–2532, Nov. 2011.
[28] Univ. Washington, Power Systems Test Case Archive, 1993 [Online]. Available: http://www.ee.washington.edu/research/pstca
[29] J. P. Deane, G. Drayton, and B. P. Ó Gallachóir, "The impact of sub-hourly modelling in power systems with significant levels of renewable generation," *Appl. Energy*, vol. 113, pp. 152–158, 2014.
[30] National Renewable Energy Laboratory, Western Wind Resources Dataset, 2006 [Online]. Available: http://wind.nrel.gov/Web_nrel/
[31] Electrical Energy Storage, Int. Electrotechnical Commission, Tech. Rep., 2011.
[32] S.-I. Inage, Prospects for Large-Scale Energy Storage in Decarbonised Power Grids, Int. Energy Agency, Tech. Rep., 2009.
[33] Beacon Power, LLC, Flywheel Energy Storage System, 2013 [Online]. Available: http://www.beaconpower.com/files/FESS_Tech_Data_Sheet.pdf
[34] IBM ILOG CPLEX Optimizer, 2012 [Online]. Available: http://www-01.ibm.com/software/integration/optimization/cplex-optimizer/
[35] A. Castillo, X. Jiang, and D. F. Gayme, "Lossy DC OPF for optimizing congested grids with renewable energy and storage," in *Proc. Amer. Control Conf.*, Portland, OR, USA, 2014.

Sonja Wogrin (M'13) received the B. S. degree in technical mathematics from the Graz University of Technology, Austria, in 2008, the M.S. degree in computation for design and optimization from the Massachusetts Institute of Technology, Cambridge, MA, USA, in 2008, and the Ph.D. degree from the Institute for Research in Technology at the Comillas Pontifical University, Madrid, Spain, in 2013.

She is now a collaborating Assistant Professor at the Comillas Pontifical University. Her research interests are decision support systems in the energy sector and optimization.

Dennice F. Gayme (M'10–SM'14) received the B.Eng. & Society degree from McMaster University, Hamilton, ON, Canada, in 1997 and the M.S. degree from the University of California at Berkeley, CA, USA, in 1998, both in mechanical engineering. In 2010, she received the Ph.D. degree in control and dynamical systems from the California Institute of Technology, Pasadena, CA, USA.

Prior to her doctoral work, she was a Senior Research Scientist at Honeywell Laboratories. In 2012, she joined the Mechanical Engineering Department at Johns Hopkins University, Baltimore, MD, USA, where she is currently an Assistant Professor. Her research interests are in analysis and control of networked and spatially distributed systems; applications include power networks and wind farms.